

# Modeling sediment transport around a rectangular bridge abutment

Hossein Basser · Ruhollah Cheraghi · Hojat Karami · Abdollah Ardeshir ·  
Mohsen Amirmojahedi · Shatirah Akib · Afshin Jahangirzadeh ·  
Shahaboddin Shamshirband

Received: 11 March 2014 / Accepted: 9 February 2015 / Published online: 24 February 2015  
© Springer Science+Business Media Dordrecht 2015

**Abstract** In the present paper, the results are explained for an experimental and numerical study on scouring phenomenon around a rectangular, impermeable and non-submerged bridge abutment cross section with perpendicular attitude to the flow axes. In this study, SSIIM 2.0 is used to simulate the scouring problem at the abutment. SSIIM 2.0 is a three-dimensional computational fluid dynamics program that uses a finite volume method to discretize the equations. According to the results, the  $k-\varepsilon$  turbulence model with some RNG extensions is the best model for predicting turbulence around the rectangular abutment. In addition, different grids are compared in the simulations and the best grid is selected based on the accuracy of numerical results and the computation times. Finally, the findings are explained, and the bed changes and local scour profiles resulting from the numerical simulation are compared with the available experimental results. It is concluded from the achieved results that SSIIM 2.0 numerical modeling is capable of simulating scouring around a rectangular abutment.

**Keywords** Abutment · Bridge · Numerical modeling · Scouring · SSIIM 2.0

---

H. Basser (✉) · M. Amirmojahedi · S. Akib · A. Jahangirzadeh  
Department of Civil Engineering, Faculty of Engineering, University of Malaya, 50603 Kuala Lumpur,  
Malaysia  
e-mail: hosseinbasser@gmail.com

R. Cheraghi · A. Ardeshir  
Department of Civil and Environmental Engineering, Amirkabir University of Technology, Tehran,  
Iran

H. Karami  
Department of Civil Engineering, Semnan University, Semnan, Iran

S. Shamshirband (✉)  
Department of Computer System and Technology, Faculty of Computer Science and Information  
Technology, University of Malaya, 50603 Kuala Lumpur, Malaysia  
e-mail: shamshirband@um.edu.my

## 1 Introduction

Bridge collapse after a flood can interrupt transport systems, threaten lives, and destroy property. In a study, Shirhole and Holt [1] claimed that over 1000 bridges have failed in the last 30 years in the United States, and 60 % of those failures were associated with scour. Bridge scour is also known for its negative impact on highway bridges in the United States [2]. The degree danger was emphasized by the results of a study conducted by the Transport Research Board, which indicated there are approximately 488,750 bridges that span streams and rivers in the United States and \$30 million are spent each year on dealing with scour-associated bridge collapses [3].

Local scour at bridges has been studied extensively over the past 50 years with both experimental and numerical methods. When an obstacle is placed in the flow on an erodible bed, a scour hole forms at the obstacle footing. In river beds, this phenomenon typically occurs in the vicinity of bridge abutments and bridge piers, often leading to the structure's collapse.

Constructing an abutment against the flow path causes hydrostatic pressure changes between the upstream and downstream of the structure, which produces a whirlpool disturbance around it. Such whirlpool flows are the main local scour mechanisms that produce large vortices in the vicinity of the abutment. Local scour mentioned above may threaten the structure's safety and lead to structural failure [4]. Whirlpool disturbance causes the formation of a primary vortex at upstream of the abutment. This primary vortex, known as downward flow, initiates the scouring process upstream of the abutment. The downward flow impinges on the stream's bed, thus instigating a scour hole in front of the abutment, which subsequently rolls up to make a complex vortex system [5]. This vortex, which is shaped like a horseshoe, is called a "horseshoe vortex". The flow separation downstream of the abutment produces wake vortices, little tornados that lift material from the streambed and generate an independent scour hole downstream of the pier [6].

Estimating the pattern of scour development and scour depth around an abutment have been considered by many researchers in recent years. Therefore, researchers have tried to predict the maximum scour depth for specific discharge in order to design proper abutment foundations. It is also necessary to know the maximum scour depth to control scour using countermeasures.

Numerous researchers such as Akib et al. (2011, 2014), Jahangirzadeh et al. (2014), Bassar et al. (2014), Dey (2005), Chiew (1992), Mashahir et al. (2004), Hua et al. (2006), Kayaturk (2004), Molinas et al. (1992), Melville (1992), and Kumar (1999) have conducted several experiments to clarify the scour phenomenon around hydraulic structures [7–19].

Since experimental modeling is not always possible and in some cases can be costly, a variety of numerical models have been developed to compute sediment transport and calculate bed changes around hydraulic structures or obstructions. SSIIM, Fluent, and Flow-3D are considered the most important numerical modeling tools for simulating sediment transport.

Recently, lots of researchers have used numerical approaches and their interest in using these methods is increasing. For example, Khosronejad et al. (2012) carried out a numerical simulation to study clear-water scour around three bridge piers with cylindrical, square, and diamond cross-sectional shapes, respectively [20]. Karami et al. (2012) performed a study to validate a numerical method of simulating the scour phenomena around a series of spur dikes [21]. Researchers including Akib et al. (2014), Khosronejad et al.

(2013), Al-Ghorab and Entesar (2013), Kang et al. (2012), and Paik et al. (2010) have also carried out other numerical studies to simulate the scouring phenomenon [22–27].

The main objective of this study is to examine the efficiency of the SSIIM 2.0 three-dimensional numerical model in estimating the local scour depth and pattern around a rectangular section abutment. This three-dimensional model was used to simulate local scour around a bridge abutment. After generating the grids, sediment transport was computed and the results were explained. Consequently, several sensitivity analyses were carried out to determine the best parameters of the numerical model.

## 2 Experimental setup

All experiments were conducted at the Porous Media Laboratory, Amirkabir University of Technology, Tehran, Iran. The flume was rectangular-section 14 m long, 1 m wide and 1 m deep. Glass was used to build the bed and flume sides. A metal frame was used to support the glass flume built. A rectangular section abutment made of glass, 0.15 m long and 0.30 m wide, was installed at a distance of 5.7 m from the flume entrance. The bed slope in the experiments was 0.0004. According to the observations, the bed sediment upstream of the abutment was not moving, and only the scoured bed around the abutment was observed. Therefore, considering the rigidity of the bed, the critical shear stress was measured based on the Shields diagram and bed sediment diameter. Establishing uniform flow and fully developed turbulent flow was ensured by measuring velocity profiles upstream of the test sections. A 25 Hz NorTek Acoustic Doppler Velocimeter (ADV) measured the velocity components. A reservoir was built at the downstream end of the flume to trap transported sediment. An inlet valve served to regulate the flow discharge and a rectangular weir was made in the flume to measure the discharge. The flow depth ( $Y$ ) was 15 cm in all experiments. To fill the flume, bed sediment ( $\sigma_g < 1.4$ ) was used, with thickness of 0.35 m, median size ( $U/U_{cr}$ ) of 0.91 mm, specific gravity ( $S_s$ ) of 2.65 and geometric standard deviation ( $\sigma_g$ ) of 1.38. The bed profile variations around the spur dikes in all tests were measured using a laser bed profiler (LBP) with  $\pm 1$  mm width accuracy and  $\pm 0.1$  mm depth accuracy. Figure 1 shows the flume and experimental abutment in the laboratory. Figure 1a depicts the physical abutment model and Fig. 1b shows the ADV and LBP in the laboratory.

Figure 2 shows a schematic view of the experimental flume and the abutment.

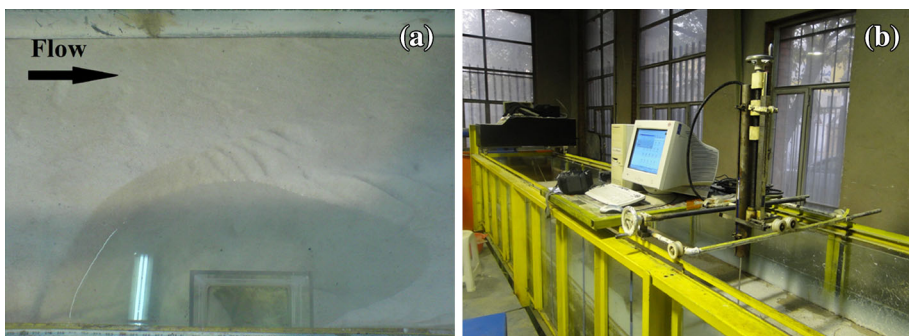


**Fig. 1** a Physical model of rectangular abutment b Acoustic Doppler Velocimeter and Laser Bed Profiler used to measure velocity and bed changes in experiments respectively

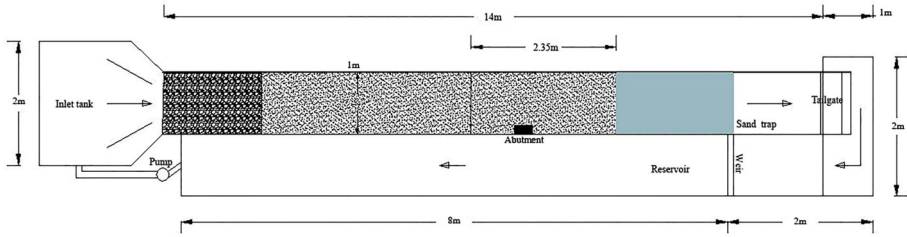


**Fig. 2** Schematic view of the flume and rectangular abutment in the laboratory

### 3 Numerical model

In this study, SSIIM 2.0, a three-dimensional computational fluid dynamics model (CFD), was used to simulate the scour phenomenon and sediment transport around a rectangular abutment. SSIIM 2.0 model utilizes a finite-volume approach to discretize equations. SSIIM 2.0 solves Reynolds-averaged Navier–Stokes equations using standard  $k-\epsilon$  and  $k-\epsilon$  turbulence model with some RNG extensions to compute water flow. In the  $k-\epsilon$  turbulence model with RNG extensions, there is an additional nonlinear term in the equation related to  $\epsilon$ , which yields more accurate results when using this equation. Also due to the additional term, this turbulence model can simulate flow over surfaces more accurately. Moreover, SSIIM 2.0 employs the SIMPLE method to compute pressure [28]. It uses a power-law scheme to discretize the convective terms. SSIIM 2.0 is capable of computing both bed load and suspended load. It computes suspended load using the transient convection–diffusion equation for sediment concentration  $c$ .

$$\frac{\partial c}{\partial t} + U_i \frac{\partial c}{\partial x_i} + w \frac{\partial c}{\partial z} = \frac{\partial}{\partial x_i} \left( \Gamma \frac{\partial c}{\partial x_i} \right) \tag{1}$$

In this equation,  $U$  is Reynolds-averaged water velocity,  $w$  is the sediment fall velocity,  $x$  is general space dimension,  $z$  is the dimension in the vertical direction, and  $\Gamma$  is the diffusion coefficient which is set equal to the eddy viscosity obtained from the  $k - \epsilon$  model [28].

Equation 1 describes sediment transport, including the effect of turbulence on decreasing the sediment settling velocity. This equation is solved using a control-volume method on all cells except the cell closest to the bed. For the cell closest to the bed, the Van Rijn (1987) formula is used to specify the concentration as follows [29]:

$$c_{bed} = 0.015 \frac{d^{0.3} \left( \frac{\tau - \tau_c}{\tau_c} \right)^{1.5}}{a \left( \frac{\rho_s - \rho_w}{\rho_w v^2} \right)^{0.1}} \tag{2}$$

In the above equation,  $d$  is sediment particle diameter,  $\tau$  is bed shear stress,  $\tau_{cr}$  is critical bed shear stress for the movement of sediment particles according to Shields’ diagram,  $\rho_w$  and  $\rho_s$  are the density of water and sediment,  $\nu$  is water viscosity and  $g$  is gravity acceleration. The critical shear stress was measured based on the Shields diagram and diameter of bed sediments.

In addition to suspended load, the bed load,  $q_b$ , is computed with the Van Rijn formula [29]:

$$\frac{q_b}{d^{1.5} \sqrt{\frac{\rho_s - \rho_w}{\rho_w} g}} = 0.053 \frac{\left(\frac{\tau - \tau_c}{\tau_c}\right)^{1.5}}{d^{0.3} \left(\frac{(\rho_s - \rho_w)g}{\rho_w v^2}\right)^{0.1}} \tag{3}$$

For applying boundary conditions, inflow and outflow discharge values are defined in the software discharge editor. The wall effect is estimated using an empirical wall function called the standard wall function [28].

$$\frac{U}{u_x} = \frac{1}{\kappa} \ln \left( \frac{30h}{k_s} \right) \tag{4}$$

where,  $k_s$  is the bed roughness,  $\kappa$  is the Prandtl constant equals to 0.4, and  $h$  is the distance from the wall.

#### 4 Validation of the numerical model

In order to validate the model’s accuracy with regard to the simulated sediment transport, four sensitivity analyses were performed to study the effect of grid, bed roughness, turbulence model, and sediment transport formula on selecting the optimum state that best agrees with the observed measurements. Based on the sensitivity analysis on bed roughness, it was determined that the amount of  $4d_{50}$  was the best roughness value for simulating scour depth around the abutment. According to a study by Olsen, the amount of bed roughness can differ from  $d_{50}$  to  $100d_{50}$  [28]. The amounts of  $d_{50}$  and  $3d_{50}$  have been proposed for bed roughness [30, 31].

Subsequently, in order to simulate the channel and abutment geometry, two structured grids were generated. The area around the abutment used a finer grid compared to the other regions due to more intense velocity gradients and also to decrease computation time. The grid sizes were  $(197 \times 21 \times 10)$  and  $(68 \times 21 \times 10)$ , with the numbers indicating the number of grids in the X, Y and Z directions respectively with distortion ratios of 0.2 and 0.5 respectively around the abutment. The distortion ratio is the dimension of the grid in one direction divided by the dimension in another direction [28]. In order to explore and compare the achieved results, two tests, namely  $R^2$  and MAE were utilized, using measured and numerical results around the abutment.

$$R^2 = 1 - \frac{\sum_{i=1}^n (E_i - N_i)^2}{\sum_{i=1}^n (E_i - \bar{E}_i)^2} \tag{5}$$

$$MAE = \frac{1}{n} \sum_{i=1}^n |E_i - N_i| \tag{6}$$

where  $E_i$  = experimental results and  $N_i$  = numerical results.

It was determined from the  $R^2$  and MAE tests that the finer grid  $(197 \times 21 \times 10)$  increases result accuracy but also significantly increases computation time. The CPU calculation time for the finer grid was 870 min, which is much higher than 220 min for the coarser grid. Since the finer grid accuracy was only 5 % higher than that of the coarser grid, the coarser grid  $(68 \times 21 \times 10)$  was selected as the optimum grid based on computation time and accuracy. Figure 3 indicates the optimum grid developed for the experimental model.

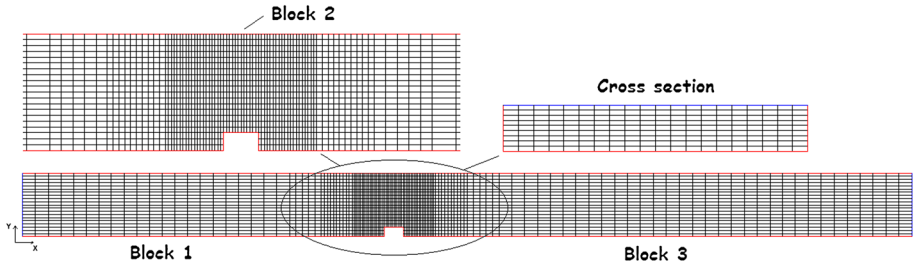


**Fig. 3** The optimum grid generated for rectangular abutment simulation

**Table 1** Comparison of the measured and simulated results and computation time for two generated grids

Grid size	Distortion ratio	MAE test results	R <sup>2</sup> test results	Computation time (min)
197 × 21 × 10	0.2	0.017314	0.87	870
68 × 21 × 10	0.5	0.018286	0.82	220

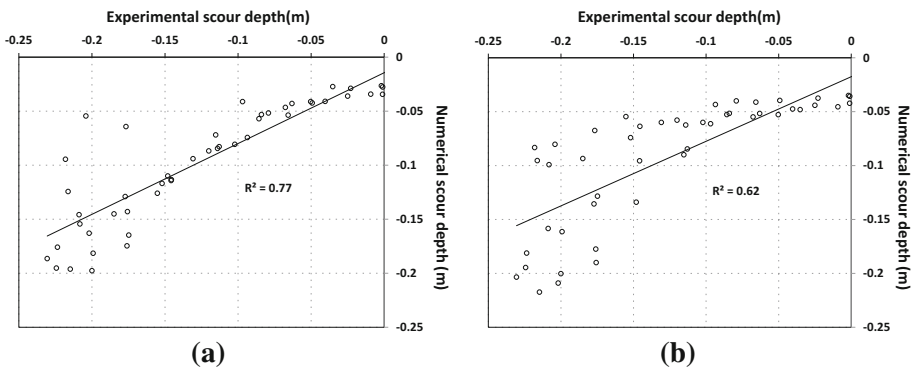


**Fig. 4** Results of R<sup>2</sup> tests for two turbulence models **a** k–ε with some RNG extensions **b** standard k–ε

Table 1 provides the duration of computations as well as the accuracy results of the R<sup>2</sup> and MAE tests for simulating scour depth in two generated grids. Fifty points around the abutment were selected for assessment in the R<sup>2</sup> and MAE test.

Next, sensitivity analysis was performed to study the effect of different turbulence models. According to the sensitivity analysis, the effect of standard k–ε and k–ε turbulence model with some RNG extensions was examined, and the latter showed the best agreement with the measured results. Figure 4 indicates the results of the R<sup>2</sup> test for comparing the measured and simulated scour depth around the abutment for both turbulence models. Also, the MAE test result showed that the k–ε turbulence model with some RNG extensions was more efficient in simulating the scouring phenomenon around the rectangular abutment. The MAE test results for standard k–ε and k–ε turbulence model with some RNG extensions were 0.021341 and 0.019225 respectively.

Moreover, sensitivity analysis was carried out to evaluate the best sediment transport formula for simulation. Based on this analysis, the results achieved from the Van Rijn formula [29] had the best agreement with the measured topography (the coefficient of

**Table 2** Comparison of results from the examined sediment transport formulas in the simulations

Sediment transport formula	R <sup>2</sup> test results	MAE test results
Experimental model	–	–
Van Rijn formula [11]	0.77	0.022
Engelund/Hansen [12]	0.32	0.057
Ackers/White formula [13]	0.37	0.053
Yang’s streampower formula [14]	0.09	0.18
Shen/Hung formula [10]	0.51	0.045
Einstein bed load formula [15]	0.14	0.011

determination, R<sup>2</sup>, for Van Rijn’s formula was around 0.77). After Van the Rijn formula, the Shen/Hung formula demonstrated good results. For sensitivity analysis, the following formulas were selected:

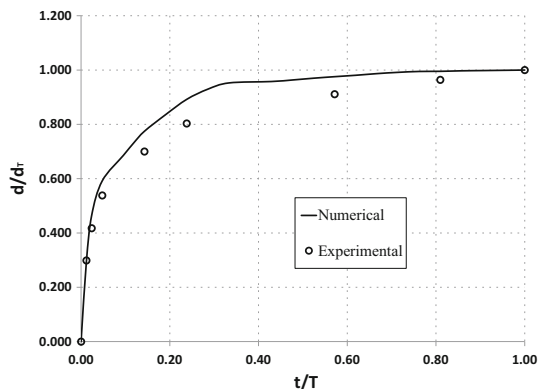
Van Rijn formula, Engelund/Hansen formula, Ackers/White formula, Yang’s stream-power formula, Shen/Hung formula, and Einstein bed load formula. Table 2 indicates the results of the R<sup>2</sup> and MAE tests.

### 5 Results and discussions

The results indicate that scouring started around the abutment at an angle of approximately 45° to the nose of the abutment. By intensifying the mechanism of scouring a horseshoe vortex formed, which transported the sediment particles downstream of the abutment. According to the observations, the scouring rate was very fast in the first hours and around 60 % of scouring occurred in the first 5 % of the experiment. It was also observed that more than 85 % of the maximum scour depth developed in the first 20 % of the experiment and computation time. Figure 5 indicates the experimental and numerical time variation of maximum scour depth. It shows that the computational results matched the experimental time variation very well.

Figure 6 illustrates the comparison of the computed and measured bed changes at sections x = 5.6 m, x = 5.7 m, x = 6.1 m and x = 6.3 m around the rectangular abutment. The graphs show acceptable accuracy of the numerical model in simulating scour phenomenon around abutments. As previously mentioned, the maximum scour depth

**Fig. 5** Comparison of the numerical and experimental variations of dimensionless maximum scour depth ( $d/d_T$ ) as a function of dimensionless time ( $t/T$ )



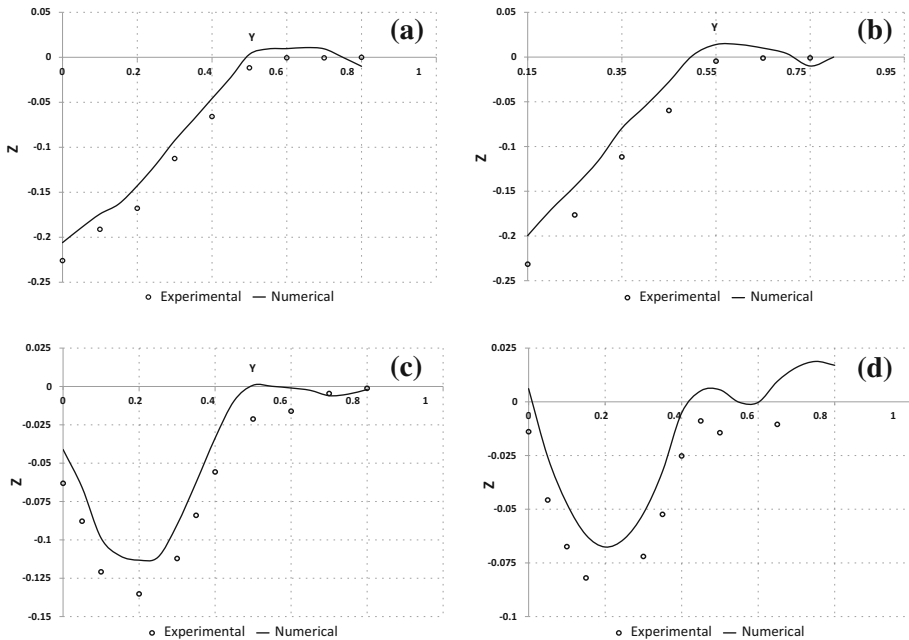


**Fig. 6** Bed changes in experimental and numerical results **a**  $x = 5.6$  m, **b**  $x = 5.7$  m, **c**  $x = 6.1$  m and **d**  $x = 6.3$  m

observed around the upstream nose of the abutment. Also, the location of the maximum scour depth was reasonably reproduced. The computational results show that the numerical model underestimated the scour depth, as the maximum scour depth was around 0.22 m in the experiments, whereas in the computation the value was 0.20 m. It is evident in Fig. 6 that there is a steep area in the cross sections, which is a result of the primary vortex that forms once the approaching flow encounters the abutment. The approaching flow encountering the abutment caused a difference in pressure between water surface and bed level, which made the flow move downward and in the opposite direction of the approaching flow. This phenomenon produced the primary vortex that signifies as the primary reason of scouring around the abutment. It is clear that scour depth decreased with moving farther away from the abutment along the channel's width. This decrease is due to the power mitigation in the primary vortex.

## 6 Conclusion

In this study, sediment transport at a rectangular abutment was investigated using experimental and numerical methods. The numerical model results showed that it is capable of modeling scouring around an abutment with sufficient accuracy. The main conclusions of this study are explained as follows:

- The distortion ratio should change softly along the grid. In addition, the results indicate that using a distortion ratio of 0.2–0.5 around the abutment led to accurate results.



- Using a finer grid just around the structure decreased the computation time significantly.
- The results obtained from using a  $k$ - $\epsilon$  turbulence model with some RNG extensions showed the best agreement with the measurements. This model is recommended for use in similar problems.
- Using the amount of  $4d_{50}$  as the roughness value led to the best agreement with experimental results in simulating scouring around a rectangular abutment.
- A comparison of the computed and measured bed changes showed that the Van Rijn sediment transport formula is the best formula to assess bed changes around a rectangular abutment. After the Van Rijn formula, the Shen/Hung formula demonstrated proper results.
- Scouring started around the abutment at an angle of approximately  $45^\circ$  to the nose of the abutment.
- It is concluded that the maximum scouring rate occurred during the first hours of the experiment and computation, and it decreased with time. 60 % and 85 % of the scouring occurred during the first 5 and 20 % of the equilibrium time, respectively.
- Maximum scour depth was observed around the upstream nose of the abutment due to the power of the primary vortices.
- The computational results signify that the numerical model underestimated the maximum scour depth by 10 %.

**Acknowledgments** The financial support of the high impact research grant from University of Malaya (UM.C/625/1/HIR/61, account number: H-16001-00-D000061) is gratefully acknowledged. The authors would also like to thank Amirkabir University of Technology for facilitating of the experiments.

## References

1. Shirhole A, Holt R (1991) Planning for a comprehensive bridge safety program. *Transp Res Rec* 1290:39–50
2. Kattell J, Eriksson M (1998) Bridge scour evaluation: screening, analysis, and countermeasures. F.S. United States Department of Agriculture, Washington
3. Lagasse PF (1997) Instrumentation for measuring scour at bridge piers and abutments. American Association of State Highway Transportation Officials National Research Council. Transportation Research Board National Cooperative Highway Research Program, National Academy Press, Washington D.C.
4. Melville BW, Coleman SE (2000) Bridge scour. Water Resources Publication, Highland
5. Karami H et al (2012) Verification of numerical study of scour around spur dikes using experimental data. *Water Environ J* 28:1–11
6. Dargahi B (1990) Controlling mechanism of local scouring. *J Hydraul Eng* 116(10):1197–1214
7. Chiew Y-M (1992) Scour protection at bridge piers. *J Hydraul Eng* 118(9):1260–1269
8. Dey S, Barbhuiya AK (2005) Time variation of scour at abutments. *J Hydraul Eng* 131(1):11–23
9. Kayaturk S, Kokpinar M, Gogus M (2004) Effect of collar on temporal development of scour around bridge abutments. In: 2nd international conference on scour and erosion, IAHR, Singapore
10. Kumar V, Raju KGR, Vittal N (1999) Reduction of local scour around bridge piers using slots and collars. *J Hydraul Eng* 125(12):1302–1305
11. Li H-MT, Kuhnle R, Barkdoll B-MT (2005) Countermeasures against scour at abutments. *Lab Publ* 49:150
12. Mashair M, Zarrati A, Rezayi A (2004) Time development of scouring around a bridge pier protected by collar. In: 2nd international conference on scour and erosion, ICSE-2, Singapore
13. Melville BW, Dongol D (1992) Bridge pier scour with debris accumulation. *J Hydraul Eng* 118(9):1306–1310
14. Molinas A, Kheireldin K, Wu B (1998) Shear stress around vertical wall abutments. *J Hydraul Eng* 124(8):822–830

15. Akib S, Jahangirzadeh A, Basser H (2014) Local scour around complex pier groups and combined piles at semi-integral bridge. *J Hydrol Hydromech* 62(2):108–116
16. Akib S et al (2011) Influence of flow shallowness on scour depth at semi-integral bridge piers. *Adv Mater Res* 243:4478–4481
17. Basser H et al (2014) Adaptive neuro-fuzzy selection of the optimal parameters of protective spur dike. *Nat Hazards* 73:1–12
18. Jahangirzadeh A et al (2014) Experimental and numerical investigation of the effect of different shapes of collars on the reduction of scour around a single bridge pier. *PLoS One* 9(6):e98592
19. Jahangirzadeh A et al (2014) A cooperative expert based support vector regression (Co-ESVR) system to determine collar dimensions around bridge pier. *Neurocomputing* 140:172–184
20. Khosronejad A, Kang S, Sotiropoulos F (2012) Experimental and computational investigation of local scour around bridge piers. *Adv Water Resour* 37:73–85
21. Karami H et al (2012) Verification of numerical study of scour around spur dikes using experimental data. *Water Environ J* 28:124–134
22. Akib S, Mohammadhassani M, Jahangirzadeh A (2014) Application of ANFIS and LR in prediction of scour depth in bridges. *Comput Fluids* 91:77–86
23. EL-Ghorab EA (2013) Reduction of scour around bridge piers using a modified method for vortex reduction. *Alexandria Engineering Journal* 52(3):467–478
24. Kang S, Khosronejad A, Sotiropoulos F (2012) Numerical simulation of turbulent flow and sediment transport processes in arbitrarily complex waterways. In: *Environmental fluid mechanics, memorial volume in honour of Prof. Gerhard H. Jirka*, CRC Press, Boca Raton, pp 123–151
25. Khosronejad A et al (2013) Computational and experimental investigation of scour past laboratory models of stream restoration rock structures. *Adv Water Resour* 54:191–207
26. Paik J, Escauriaza C, Sotiropoulos F (2010) Coherent structure dynamics in turbulent flows past in-stream structures: some insights gained via numerical simulation. *J Hydraul Eng* 136(12):981–993
27. Khosronejad A et al (2011) Curvilinear immersed boundary method for simulating coupled flow and bed morphodynamic interactions due to sediment transport phenomena. *Adv Water Resour* 34(7):829–843
28. Olsen NRB (2006) A three-dimensional numerical model for simulation of sediment movements in water intakes with multiblock option. User's manual
29. Van Rijn LC (1987) Mathematical modelling of morphological processes in the case of suspended sediment transport. *Waterloopkundig Laboratorium, Delft*
30. Wu W, Rodi W, Wenka T (2000) 3D numerical modeling of flow and sediment transport in open channels. *J Hydraul Eng* 126(1):4–15
31. Khosronejad A et al (2007) 3D numerical modeling of flow and sediment transport in laboratory channel bends. *J Hydraul Eng* 133(10):1123–1134